

Maria L. Golson,^{1,2} Jennifer C. Dunn,^{1,2} Matthew F. Maulis,^{1,2} Prasanna K. Dadi,³ Anna B. Osipovich,^{3,4} Mark A. Magnuson,^{3,4} David A. Jacobson,³ and Maureen Gannon^{1,2,3,5}



Activation of FoxM1 Revitalizes the Replicative Potential of Aged β -Cells in Male Mice and Enhances Insulin Secretion

Diabetes 2015;64:3829–3838 | DOI: 10.2337/db15-0465

Type 2 diabetes incidence increases with age, while β -cell replication declines. The transcription factor FoxM1 is required for β -cell replication in various situations, and its expression declines with age. We hypothesized that increased FoxM1 activity in aged β -cells would rejuvenate proliferation. Induction of an activated form of FoxM1 was sufficient to increase β -cell mass and proliferation in 12-month-old male mice after just 2 weeks. Unexpectedly, at 2 months of age, induction of activated FoxM1 in male mice improved glucose homeostasis with unchanged β -cell mass. Cells expressing activated FoxM1 demonstrated enhanced glucose-stimulated Ca^{2+} influx, which resulted in improved glucose tolerance through enhanced β -cell function. Conversely, our laboratory has previously demonstrated that mice lacking FoxM1 in the pancreas display glucose intolerance or diabetes with only a 60% reduction in β -cell mass, suggesting that the loss of FoxM1 is detrimental to β -cell function. Ex vivo insulin secretion was therefore examined in size-matched islets from young mice lacking FoxM1 in β -cells. Foxm1-deficient islets indeed displayed reduced insulin secretion. Our studies reveal that activated FoxM1 increases β -cell replication while simultaneously enhancing insulin secretion and improving glucose homeostasis, making FoxM1 an attractive therapeutic target for diabetes.

Diabetes afflicts 347 million people worldwide (1) and is associated with reduced functional β -cell mass (2,3). The incidence of diabetes in the U.S. has increased from less

than 5% in people between 20 and 44 years of age to more than 25% in people older than 65 (4). The increased incidence of diabetes with age inversely correlates with β -cell proliferation (5–7), the primary mechanism for increasing β -cell mass after early postnatal life (5,8).

Mouse models confirm that β -cell replication decreases with age (9,10). Proliferation is highest before sexual maturity in mice and in humans and continues to decline throughout adulthood. In addition to a decline in baseline replication, the ability of β -cells to respond to proliferative stimuli also diminishes with age. In mice at 2 months of age, pregnancy, streptozotocin treatment, high-fat diet, treatment with the glucagon-like peptide 1 receptor analog exendin-4, and partial pancreatectomy all potently increase β -cell replication (9,11). By 8 months of age, however, only partial pancreatectomy can stimulate β -cell proliferation, and by 14 months of age, none of these stimuli are able to increase β -cell replication over baseline. A goal for treating type 2 diabetes (T2D), therefore, is to induce replication in endogenous β -cells. However, dividing β -cells often display suboptimal performance (12), so simply increasing proliferation may not result in increased functional β -cell mass. Ideal therapies for diabetes would both expand β -cell mass and enhance insulin secretion.

A partial explanation for the diminution in β -cell proliferation with age is an accumulation of the cell-cycle inhibitor p16^{Ink4a}, encoded by *Cdkn2a*, in aged β -cells (10). Overexpression of p16 in young, nonstimulated mice decreases baseline β -cell proliferation to that observed

¹VA Tennessee Valley Healthcare System, Nashville, TN

²Division of Diabetes, Endocrinology, and Metabolism, Department of Medicine, Vanderbilt University School of Medicine, Nashville, TN

³Department of Molecular Physiology and Biophysics, Vanderbilt University School of Medicine, Nashville, TN

⁴Vanderbilt Center for Stem Cell Biology, Vanderbilt University Medical Center, Nashville, TN

⁵Department of Cell and Developmental Biology, Vanderbilt University School of Medicine, Nashville, TN

Corresponding author: Maureen Gannon, maureen.gannon@vanderbilt.edu.

Received 6 April 2015 and accepted 26 July 2015.

This article contains Supplementary Data online at <http://diabetes.diabetesjournals.org/lookup/suppl/doi:10.2337/db15-0465/-/DC1>.

© 2015 by the American Diabetes Association. Readers may use this article as long as the work is properly cited, the use is educational and not for profit, and the work is not altered.

in much older mice but has no effect on β -cell division in older mice; conversely, loss of p16 increases proliferation in aged β -cells to levels observed in young mice but has no effect on β -cell proliferation in young mice. The transcription factor FoxM1 indirectly negatively regulates *Cdkn2a* through activation of *c-Myc* and *Bmi1* (13,14). FoxM1 is required for β -cell proliferation in several situations, including postnatal growth, pregnancy, and partial pancreatectomy (15–17). Deletion of *Foxm1* in the pancreas manifests post-weaning as a 60% deficit in β -cell mass accompanied by diabetes or glucose intolerance in male mice (15).

Full-length FoxM1 is required for β -cell proliferation but is not sufficient to promote β -cell proliferation in young mice, even in response to the replicative stimulus of 60% partial pancreatectomy (17). The inability of full-length FoxM1 to promote β -cell division likely results from posttranslational regulation of FoxM1 activity. Previous work suggests that transduction of human islets by full-length FOXM1 can increase β -cell replication. However, this work was performed *ex vivo*, and β -cell replication may have been affected by growth factors in the media that are not present *in vivo* (18). We therefore used a mouse model we derived in which an activated form of FoxM1 lacking its N-terminal intramolecular repressor domain can be induced specifically in β -cells by doxycycline (Dox) treatment (referred to as β -FoxM1* mice) (19). After 2 weeks of activated FoxM1 expression in aged mice, β -cell mass and proliferation as well as glucose homeostasis were examined. Our results demonstrate that activated FoxM1 can counteract the age-related decline in β -cell replication and highlight an unappreciated role for FoxM1 in enhancing insulin secretion. Altogether, these experiments suggest FoxM1 as a novel therapeutic target for simultaneously enhancing β -cell mass and function to treat diabetes.

RESEARCH DESIGN AND METHODS

Mice

RIP-rtTA (20), HA-TetO-FoxM1 ^{Δ NRD} (19), RIP-Cre (21), and *Foxm1*^{*fl*} (22) mice have been described previously. RIP-rtTA mice were maintained on a C57Bl6/J background, HA-TetO-FoxM1 ^{Δ NRD10} and HA-TetO-FoxM1 ^{Δ NRD14} mice were maintained on a C57Bl6/JxDBA mixed background, RIP-Cre and *Foxm1*^{*fl*} mice were maintained on a mixed C57Bl6/JxDBAx129Sve background, and *Foxm1*^{*LCA*} mice were maintained on a mixed C57Bl6/Jx129Sve background. Mice were housed in a controlled-temperature environment with a 12-h light/dark cycle. All experiments were performed on male mice except when examining mice on postnatal day 8 (P8) mice, when both sexes were used, and for *Foxm1* and target gene expression analysis, when female C57Bl6/J mice were used. Experimental mice or dams were administered water containing 2% Dox supplemented with sucralose (2 weeks for experimental mice and from embryonic day [E] 9.5 to P8 for dams). All procedures were approved and performed in accordance with the Vanderbilt Institutional Animal Care and Use Committee.

The *Foxm1*^{*LCA*} allele was generated using bacterial artificial chromosome recombineering, which is described in detail by Chen et al. (23). Briefly, ~500 bp regions of homology ~6 Kb upstream and ~11 Kb downstream from the *Foxm1* transcriptional start site (regions “A” and “D” in Supplementary Fig. 1A) were amplified by PCR from the bacterial artificial chromosome bMQ-387I22 (Geneservice) and cloned into the HindIII and NotI sites of pBS-DTA using standard procedures. PmeI and SmaI sites were added in the NotI site. This new plasmid with regions of *Foxm1* homology was recombined using EL350 cells into bMQ-387I22 (Geneservice) to replace exons 2–4 with a selection cassette encoding pu Δ TK and neomycin (Supplementary Fig. 1A). Approximately 500 bp sequences of *Foxm1* 1.3 Kb upstream and 8 Kb downstream of the *Foxm1* transcriptional start site (regions “B” and “C” in Supplementary Fig. 1A) were cloned into pLCA.71.2272NTK+XhoI. This vector was used to retrieve the modified *Foxm1* sequence through recombination in EL350 cells. The resulting plasmid was then linearized with SmaI and electroporated into 129Sve embryonic stem cells, which were positively selected with neomycin and negatively selected with ganciclovir. Electroporation and antibiotic selection were performed by the Vanderbilt Transgenic/ES Cell Shared Resource.

Surviving cells were screened by Southern blot analysis after digesting embryonic stem cell DNA with XhoI and probing with a fragment of outside of the 5' region of homology (indicated by bar 5' of “A” in Supplementary Fig. 1A). Untargeted clones yielded a 20-Kb fragment, and correctly targeted clones yielded a 9-Kb fragment. Positive clones were rescreened with the same digest/probe combination and also by digesting with FspI and probing for sequences outside the 3' region of homology (probe represented by bar 3' of “D” in Supplementary Fig. 1A), which yielded fragments of 23 Kb wild type (WT) and 12 Kb (targeted). Southern blot probes were made by cloning ~500 bp regions of *Foxm1* approximately into pCR2.1 using the TOPO-TA cloning kit (Invitrogen) and excising them with EcoRI. Southern blotting was performed as previously described (24).

Of 114 colonies, 3 (2, 5, and 6 in Supplementary Fig. 1B) displayed the correct banding pattern at both the 5' and 3' ends. Clone 6, with 40% normal karyotype, was selected to expand and inject into blastocysts. Two 90% male chimeras achieved germline transmission. Mice were genotyped using PCR with the following primers: 5'-CTA GTG GTT GAT CTC ACC AGT, 5'-TGT GGC ATG TGG GTC AAT CCT, and 5'-TAC CGG TGG ATG TGG AAT GTG. All other primer sequences are available upon request.

Immunolabeling and Morphometry

Tissue was processed as previously described (25). Measurements of β -cell mass were performed, as previously described, on slides through the entire pancreas 250 μ m apart, resulting in 6–12 slides per mouse (25). Slides were imaged with a ScanScope CS or FL (Leica Biosystems) or

with a LSM 710 META Inverted confocal microscope (Carl Zeiss) for H2AX immunolabeling. Cell counts were performed manually on three sections 500 μm apart, as previously described (19); cell counts per mouse per experiment ranged from at least 5,000 to $>75,000$. Cell size was calculated as previously described (19). Islet size distribution was measured by circling islets on sections used for β -cell mass assessment within ImageScope software (Leica Biosystems), which automatically displays areas of islets. Proliferation assessments within islets sorted by size were performed manually and normalized to the total β -cell area for the islets within the bin size because large islets comprised much more total area than small islets.

Antibodies used were guinea pig anti-insulin (1:500–1:1,000; Dako), mouse anti-p16 (1:50–1:100; Santa Cruz Biotechnology), mouse anti-HA (1:50–1:100; Cell Signaling Technology), rabbit anti- γ -H2AX (1:500; Cell Signaling Technology), rabbit anti-FoxM1 (1:500–1:1,000; Santa Cruz Biotechnology), rabbit anti-Ki67 (1:500; BD Biosciences), Alexa 488–conjugated mouse anti-HA (1:50; Cell Signaling Technology), horseradish peroxidase–conjugated donkey anti-guinea pig (1:400; The Jackson Laboratory), Alexa 488–conjugated donkey anti-guinea pig (1:400; The Jackson Laboratory), Alexa 647–conjugated donkey anti-guinea pig (1:400; The Jackson Laboratory), Alexa 555–conjugated anti-rabbit (1:400; The Jackson Laboratory), and Alexa 555–conjugated anti-mouse (1:400; The Jackson Laboratory).

Immunohistochemistry and immunofluorescence were performed, as previously described (19), with the following exceptions: 1) HA, Ki67, and p16 immunolabeling required citric acid buffer antigen retrieval; 2) for HA immunolabeling, overnight incubation occurred at room temperature, and 3) because p16 immunolabeling was oversaturated with incubation at room temperature, p16 and HA incubation occurred sequentially rather than in parallel. For p16/HA double-labeling, mouse anti-p16 labeled with a Zenon mouse Ig2a Alexa 555 kit (Life Technologies) and a direct Alexa 488–labeled mouse anti-HA antibody (1:50, Santa Cruz Biotechnology) were used. To examine embryonic heart and liver structure and to nonquantitatively assess DNA content, sections were labeled with 0.5 $\mu\text{g}/\text{mL}$ DAPI for 1 minute.

Quantitative Real-Time PCR

RNA extractions and quantitative PCR were performed as previously described (19).

Cytoplasmic Calcium Measurements

Islets from β -FoxM1^{*14} mice were dispersed with 0.05% trypsin after incubation overnight in RPMI medium containing 15% FBS and 2 $\mu\text{g}/\text{mL}$ Dox. Dispersed islets were incubated (20 min at 37°C) in Krebs-Ringer buffer supplemented with 2 $\mu\text{mol}/\text{mL}$ fura-2 acetoxyethyl ester (Molecular Probes). Fluorescence imaging was performed using a Nikon Eclipse TE2000-U microscope equipped with an epifluorescence illuminator (Sutter Instrument Company), a charge-coupled device camera (CoolSNAP HQ2; Photometrics), and Nikon

Elements software. Cells were perfused at 37°C at 2 mL/min with Krebs-Ringer buffer solutions that contained 2 mmol/L (first 3 min) or 14 mmol/L glucose (next 22 min). The ratios of emitted fluorescence intensities at excitation wavelengths of 340 and 380 nm (F340/F380) were determined every 5 s. Ca^{2+} imaging was followed by immunolabeling for insulin and the HA-tag on activated FoxM1; after imaging, single cells that expressed activated FoxM1 were compared with those that did not.

Metabolic Assays

Intraperitoneal glucose tolerance tests (IP-GTT) were performed as previously described (26). For insulin measurement during the IP-GTT, blood was collected from the saphenous vein, and insulin content was measured by the Vanderbilt Hormone Assay & Analytical Services Core. For insulin tolerance tests, mice were fasted for 6 h, blood glucose was measured, and mice were injected with insulin at 0.8 units/kg body weight. Blood glucose was measured periodically for 90 min.

Statistics

All data are plotted as mean \pm SEM. One-way ANOVA, two-way ANOVA, two-way ANOVA with repeated measures, with Tukey or Bonferroni posttests, or the Student *t* test were used to analyze data, as appropriate. One-way ANOVA was used to assess liver and heart size, and the χ^2 test was used to evaluate viability of the *Foxm1*^{LCA} lineage. *P* values <0.05 were considered significant.

RESULTS

Foxm1 and Target Expression Decline With Age

Because FoxM1 indirectly negatively regulates p16 (13,14) and p16 accumulates with age, we predicted that expression of *Foxm1* and its direct targets would decline with age. We therefore examined expression of *Foxm1*, *S-phase associated kinase 2* (*Skp2*), and *Aurora B kinase* (*Aurbk*) in islets from 2-, 4-, 8-, and 12-month-old mice. A significant decline in *Foxm1* was apparent as early as 4 months of age. By 12 months of age, all three proliferation-associated genes were significantly downregulated (Fig. 1).

β -Cell Mass and Proliferation Increase in Aged Mice Expressing Activated FoxM1

We hypothesized that restoring FoxM1 activity in aged β -cells would rejuvenate their replicative potential. Control (RIP-rtTA) and β -FoxM1* embryos were exposed to Dox to induce expression of activated FoxM1 beginning at embryonic day (E)9.5, just after the pancreas starts to form. β -FoxM1* mice exhibited no change in β -cell mass or ad libitum-fed blood glucose at postnatal day (P)8 (Fig. 2A–D). Similarly, when 8-week-old β -FoxM1* mice were treated with Dox for 2 weeks, there was no change in β -cell mass or proliferation compared with controls (Fig. 2E–H).

However, at 4, 8, and 12 months of age, β -cell mass was increased in β -FoxM1* mice after only 2 weeks of activated FoxM1 induction (Fig. 3A, D, and E). Because

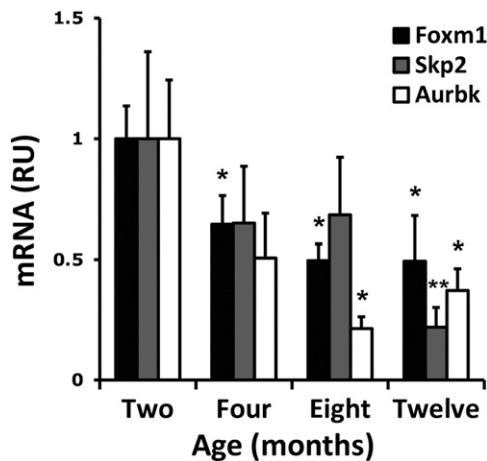


Figure 1—Quantitative real-time PCR reveals that expression of *Foxm1* and its direct targets declines with age. RU, relative units. * $P < 0.05$ vs. 2-month islets; ** $P < 0.01$ vs. 2-month islets.

of the marked increase in β -cell mass and the known recalcitrance of β -cells to proliferative stimuli at 12 months of age, we focused our attention on this time point for further study.

β -Cell proliferation was also increased at 12 months of age after 2 weeks of FoxM1 induction (Fig. 3B, F, and G). Although a trend toward increased β -cell proliferation was apparent in islets of all sizes, robust and significant increases in β -cell proliferation were apparent only in islets smaller than 1000 μm (Fig. 3H). No significant difference in islet size (Supplementary Fig. 2) or the number of individual β -cells located near ducts (0.022 ± 0.003 for RIP-rtTA mice and 0.029 ± 0.012 in β -FoxM1* mice) was observed between the two genotypes. A trend toward increased numbers of islets in the smallest and largest bins, however, may explain the overall increase in β -cell mass in β -FoxM1* mice. The lack of difference in β -cell size in β -FoxM1* mice (Fig. 3I) supports β -cell proliferation

as the mechanism by which β -cell mass increased in β -FoxM1* mice.

Our previous studies revealed that activated FoxM1 can be detected in $\sim 10\%$ of β -cells at any given time, yet robust proliferation and β -mass expansion was observed. These results suggested that FoxM1 activation might result in non-cell-autonomous effects on β -cell proliferation. Expression of activated FoxM1 was examined in proliferating and nonproliferating β -cells (Fig. 3C, J, and K). A higher percentage of FoxM1*-expressing cells replicate than cells lacking activated FoxM1, indicating that FoxM1 is acting in a cell-autonomous manner, consistent with its known role in transactivating cell-cycle genes (14,22,27). The lower overall replication in Fig. 3C compared with Fig. 3B results from the different labeling conditions used.

Activated FoxM1 Bypasses p16 to Reactivate the Cell Cycle in Aged β -Cells

Because FoxM1 inhibits expression of *Cdkn2a*, p16 expression was examined in aged β -FoxM1* mice. As has been reported previously (11,28), p16 could be observed in nearly all β -cells at 12 months of age in control mice (data not shown), and this was also true in β -FoxM1* mice, even in β -cells expressing activated FoxM1 (Fig. 4A and B), indicating that increased β -cell replication in aged β -FoxM1* mice does not result from decreased p16. Another marker of cell-cycle arrest, phosphorylated histone H2AX (γ -H2AX) (29) was, however, significantly downregulated in β -FoxM1* mice (Fig. 4C–E). Because γ -H2AX is also a marker of DNA damage, we assayed for TUNEL+ β -cells but did not observe any in control or β -FoxM1* mice ($n = 6$; 3 slides per mouse), indicating that activated FoxM1 may bypass p16 to overcome cell-cycle arrest and activate cell-cycle progression.

FoxM1 Regulates β -Cell Function

Increased β -cell mass may not be sufficient to improve insulin secretion or glucose homeostasis because increased β -cell replication is sometimes associated with decreased

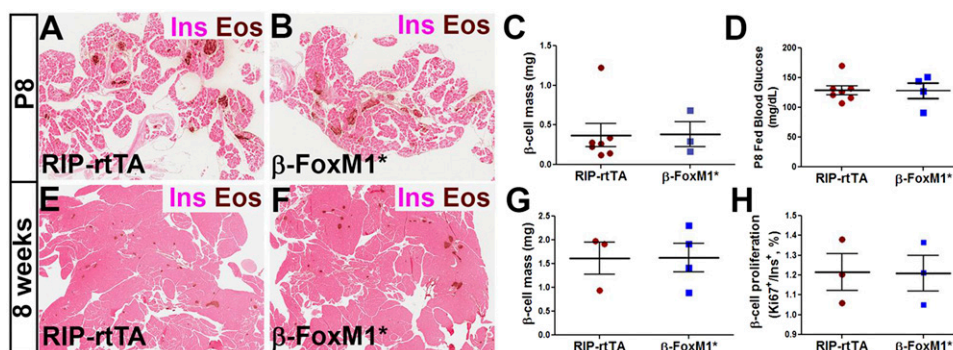


Figure 2— β -Cell mass in young mice does not increase in response to increased FoxM1 activity. Insulin labeling and eosin (EOS) staining on P8 RIP-rtTA (A) and β -FoxM1* (B) pancreas sections. C: Quantification of P8 β -cell mass. D: Ad libitum-fed glucose in P8 mice. Insulin labeling and eosin staining on 2-month old RIP-rtTA (E) and β -FoxM1* (F) pancreas sections. Quantification of β -cell mass (G) and proliferation (H) in 2-month-old mice.

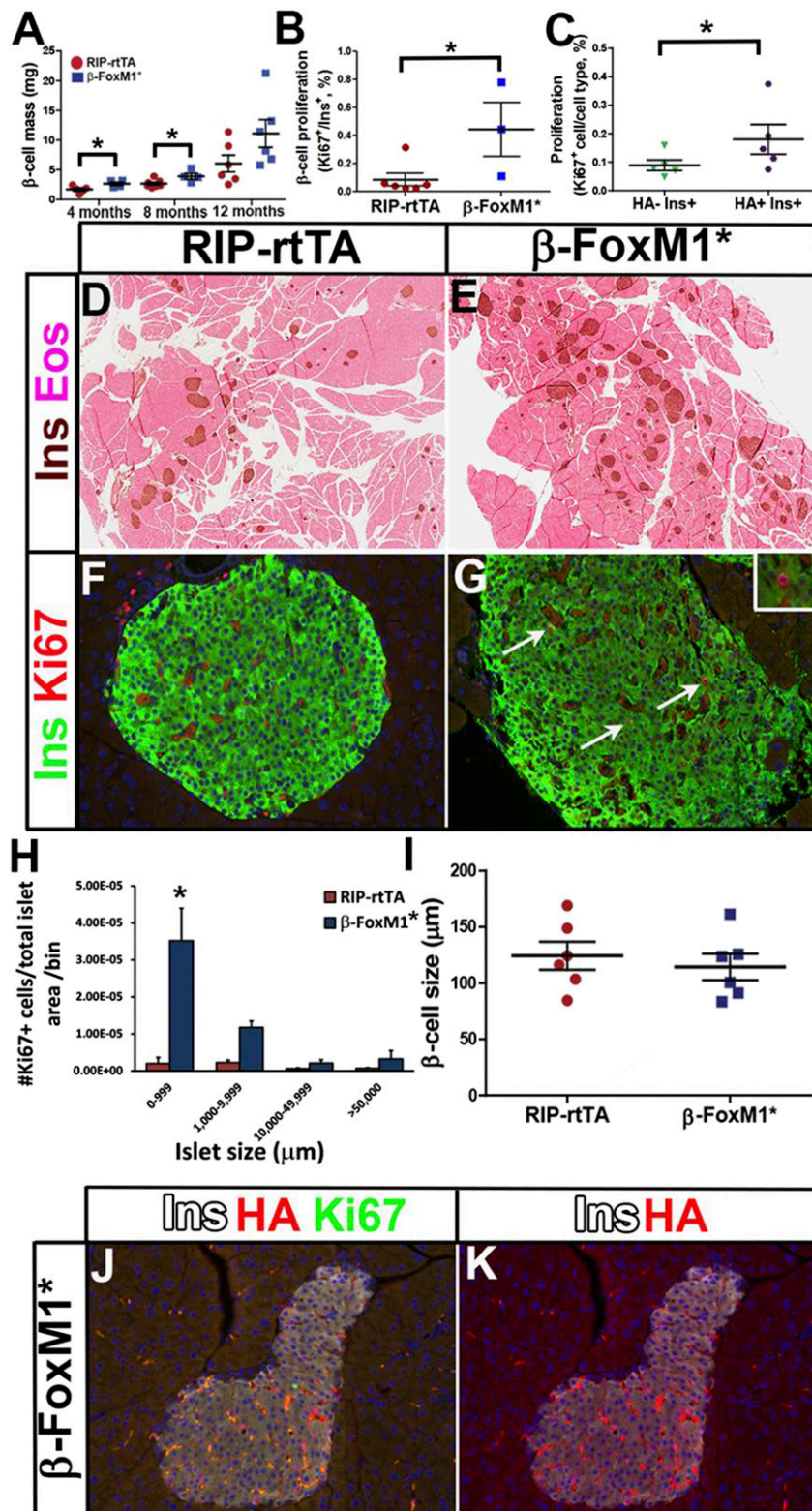


Figure 3—β-Cell mass and proliferation increase in aged mice expressing activated FoxM1. **A**: β-Cell mass in aging mice. **B**: β-Cell proliferation in 12-month-old mice. **C**: Quantification of Ki67 in activated FoxM1-expressing (HA⁺) or activated FoxM1-absent (HA⁻) β-cells at 12 months of age. **D–G**: Representative images for data quantified in **A** and **B**. Insulin (Ins) labeling and eosin (EOS) staining (**D** and **E**) and insulin and Ki67 labeling (**F** and **G**) on 12-month-old RIP-rtTA (**D** and **F**) and β-FoxM1* (**E** and **G**) pancreas sections. The arrows indicate positive cells. Images in **F** and **G** were acquired at original magnification ×200. Inset in **G** shows a higher-resolution Ki67⁺ β-cell. **H**: β-Cell size in 12-month-old mice. **I**: Proliferation in size-sorted islets. **J** and **K**: Representative image of data quantified in **C** with all three immunolabels (**J**) or with only insulin and HA immunolabels (**K**). **P* < 0.05.

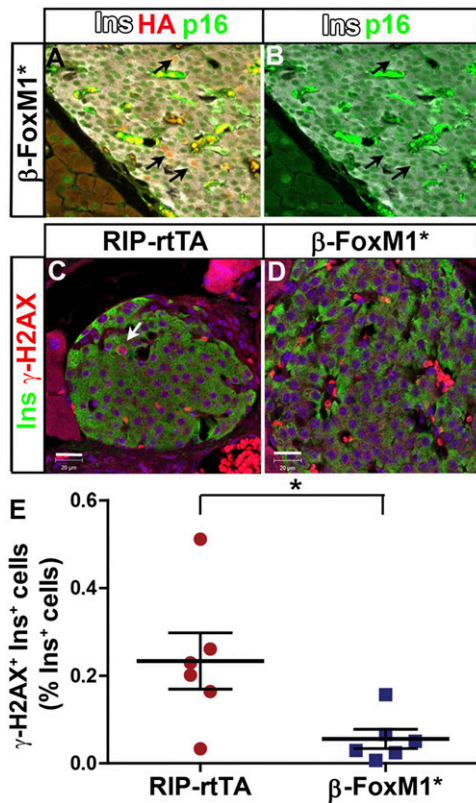


Figure 4—FoxM1 decreases γ -H2AX with no change in p16. **A:** Insulin (Ins), HA, and p16 labeling on 12-month-old and β -FoxM1* pancreas sections. **B:** Single-channel labeling of p16 from image in **A**. The black arrows indicate β -cells positive for p16 and activated FoxM1. Images were acquired at original magnification $\times 200$. Insulin and γ -H2AX labeling on RIP-rtTA (**C**) and β -FoxM1* (**D**) pancreas sections. The white arrow indicates a cell positive for insulin and γ -H2AX. **E:** Quantification of γ -H2AX+ β -cells. Scale bar: 20 μ m. * $P < 0.05$.

β -cell function (12). We therefore examined glucose homeostasis in β -FoxM1* mice. At 2 months of age, before any change in β -cell mass, β -FoxM1* mice exhibited improved glucose tolerance after receiving Dox, but no change was observed in RIP-rtTA mice (Fig. 5A and B). Ad libitum-fed blood glucose was normal (Fig. 5C). No difference was observed in insulin secretion during a glucose tolerance test (data not shown). No difference was observed in insulin tolerance between β -FoxM1* mice and RIP-rtTA mice (Fig. 5D), implying that the difference in glucose tolerance is a result of enhanced β -cell function. The improvement in glucose tolerance was still observed in 12-month-old β -FoxM1* mice (Fig. 5E and F), with no change in ad libitum-fed blood glucose (Fig. 5G).

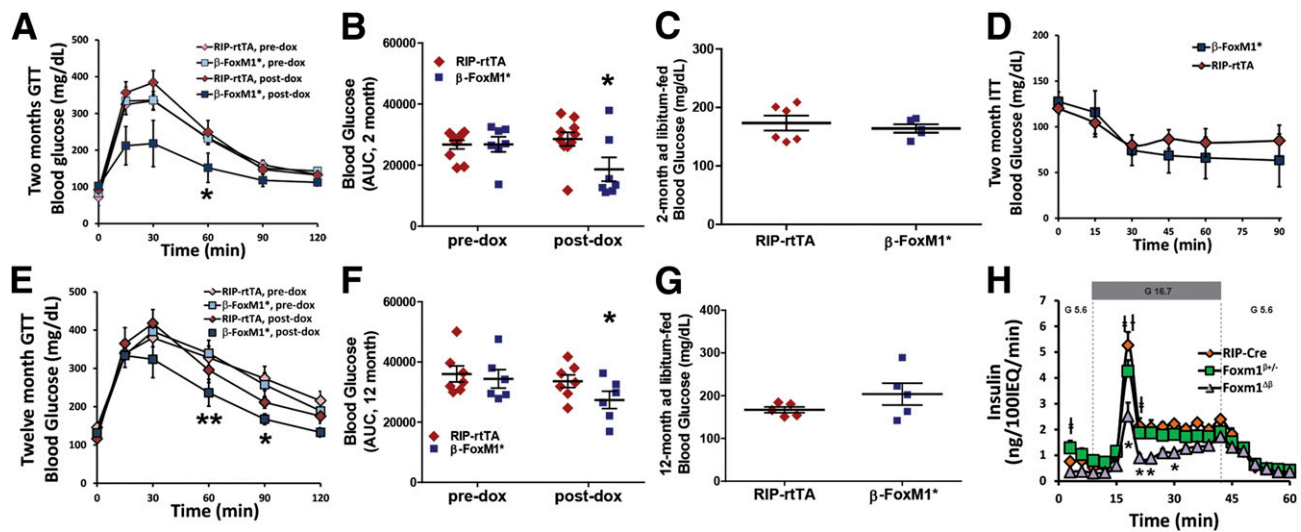
To determine whether the effect on β -cell function was due to a neomorphic trait of activated FoxM1 or an endogenous role of FoxM1, perfusions were performed on size-matched islets from RIP-Cre mice, mice lacking FoxM1 in β -cells (RIP-Cre;Foxm1^{fl/fl} mice, referred to as Foxm1^{Δβ} mice), and mice lacking one copy of Foxm1 in the

β -cell (RIP-Cre;Foxm1^{fl/fl} mice, referred to as Foxm1^{β+/-} mice). RIP-Cre mice were used as controls because they display impaired glucose-stimulated insulin secretion (GSIS) compared with mice with no Cre expression (data not shown); a deleterious effect of the RIP-Cre transgene on β -cell function has been reported previously (30,31). Size-matched islets are necessary because mice lacking Foxm1 have decreased β -cell mass (15). Islets from Foxm1^{Δβ} mice exhibited impaired GSIS compared with RIP-Cre and Foxm1^{β+/-} mice (Fig. 5H), indicating that FoxM1 has an endogenous role in regulating β -cell function. Size-matched islets from Foxm1^{Δβ} mice had normal insulin content (data not shown), suggesting that the defect in β -cell function lies downstream of insulin production.

To further determine where in the GSIS pathway FoxM1 exerts its regulatory effects and whether FoxM1 is acting cell autonomously, glucose-stimulated Ca²⁺ entry into dispersed β -cells from β -FoxM1*¹⁴ mice (19) was assessed. When glucose enters the β -cell, metabolic action causes an increased ATP-to-ADP ratio; this leads to closure of the ATP-dependent K⁺ channel and depolarization of the β -cell membrane potential, allowing increased Ca²⁺ influx. Ca²⁺ influx into β -cells causes insulin granules to fuse to the plasma membrane and release their insulin (32). Interestingly, cells expressing activated FoxM1 (HA⁺ cells) displayed increased Ca²⁺ influx during the time corresponding to the second phase of insulin secretion compared with cells not expressing activated FoxM1 (HA⁻ cells) (Fig. 6A: average traces; Fig. 6B: representative individual traces; and Fig. 6C: area under the curve for indicated time points), indicating that the effect of insulin secretion is cell autonomous. Observing this effect at the level of Ca²⁺ influx indicates that the enhancement of β -cell function achieved by increased FoxM1 activity occurs upstream of Ca²⁺ influx.

FoxM1 Is Expressed at Lower Levels in Quiescent and Proliferating Islet Cells

In most cell types, FoxM1 protein expression can only be detected in proliferating cells (33) and is rapidly degraded after cytokinesis (34). Our data suggest that FoxM1 plays an important role in nonproliferating β -cells to promote β -cell function. To characterize the FoxM1 expression pattern in highly proliferative islets, we immunolabeled pancreas sections from Lep^{ob/ob} mice, which show β -cell hyperplasia in response to leptin deficiency and insulin resistance (35). We tested the specificity of the FoxM1 antibody on Foxm1^{LCA/LCA} embryos (Fig. 7A–D), a Foxm1-null mouse we recently generated (Supplementary Fig. 1). Foxm1^{LCA/LCA} mice recapitulate the phenotype of Foxm1^{-/-} mice (36): no Foxm1^{LCA/LCA} mice survive to birth (0 of 25; $\chi^2 = 8.360$; $P = 0.0153$), and the number of Foxm1^{LCA/LCA} mice is reduced at E15.5 (7 of 53; $\chi^2 = 3.931$; $P = 0.0474$). Foxm1^{LCA/LCA} embryos display increased numbers of cells with endoreplication in heart and liver at E15.5 (Supplementary Fig. 3), and liver weight is significantly reduced (Supplementary Fig. 4).



FoxM1 was nuclear in the developing heart (Fig. 7A), but appeared cytoplasmic in the E15.5 pancreas (Fig. 7C). Sequestration of FoxM1 in the cytoplasm has been reported as a way of controlling FoxM1 activity (37). Importantly, neither nuclear nor cytoplasmic reactivity was observed in heart (Fig. 7B) or pancreas (Fig. 7D) from $Foxm1$ -null embryos.

Unlike many other cell types (33,34), we found that all endocrine cells express FoxM1 in adult $Lep^{ob/ob}$ mice (Fig. 7E–H). Most endocrine cells expressed low levels of FoxM1 (FoxM1^{LO} cells), but a few showed higher expression (FoxM1^{HI} cells; Fig. 7E). FoxM1^{HI} endocrine cells exhibited similar FoxM1 levels as the rare FoxM1⁺ exocrine cells (Fig. 7F). All of the FoxM1^{HI} endocrine cells expressed the proliferation marker Ki67 (Fig. 7G), as did all FoxM1-expressing

acinar cells (Fig. 7H). In addition, RNA-Seq of sorted quiescent and cycling β -cells using CyclinB1-GFP revealed low levels of $Foxm1$ expression in nonproliferating β -cells compared with cycling β -cells (19 fragments per kilobase of exon per million fragments mapped (FpkM) in quiescent cells vs. 1,532 FpkM in proliferative cells; personal communication from Y. Dor). Thus, FoxM1^{LO} cells appear to be nonproliferative, suggesting that lower levels of FoxM1 are sufficient to promote β -cell function, whereas higher levels of FoxM1 are associated with proliferation.

DISCUSSION

We demonstrate that expression of activated FoxM1 in aged β -cells triggers cell-cycle progression, leading to

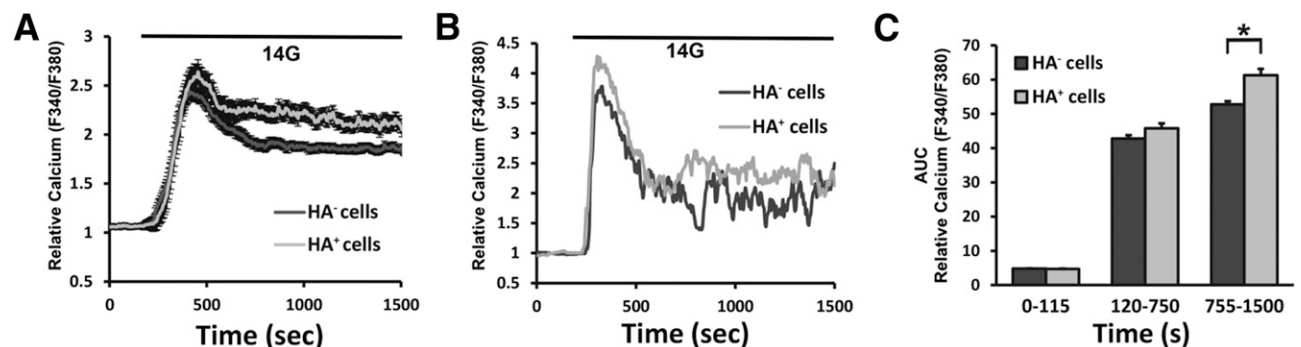


Figure 6—FoxM1 acts cell autonomously to enhance calcium influx upstream of insulin secretion. **A**: Average calcium measurements from β -FoxM1⁺ β -cells from mice expressing or lacking activated FoxM1. Dispersed β -cells were maintained in 2 mmol/L glucose until 180 s, when they were treated with 14 mmol/L glucose. **B**: Representative calcium traces from individual cells. **C**: Area under the curve (AUC) for HA⁺ and HA⁻ cells for indicated time period ($n = 2$ mice, 24–98 cells). * $P < 0.0005$.

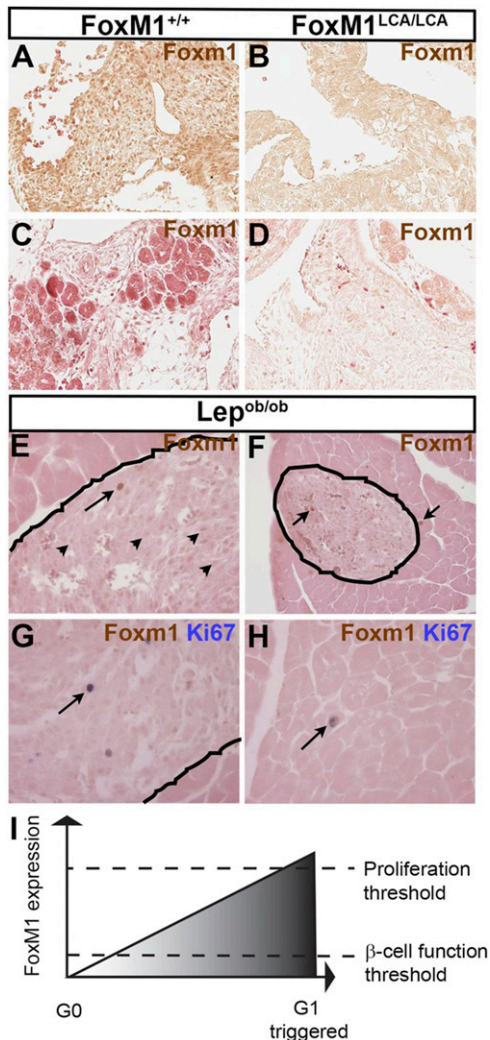


Figure 7—FoxM1 is more highly expressed in proliferating β -cells. FoxM1 immunohistochemistry on E15.5 WT (A and C) and FoxM1-null (B and D) hearts (A and B) and pancreas (C and D). E–H: FoxM1 immunohistochemistry on *Lep^{ob/ob}* pancreas sections. The lines denote boundaries between islet and exocrine tissue. E: The arrowheads indicate some FoxM1^L islet cells; the arrow indicates a FoxM1^H islet cell (original magnification $\times 200$). F: The arrows indicate FoxM1^H cells (original magnification $\times 100$). FoxM1 and Ki67 double immunohistochemistry on *Lep^{ob/ob}* pancreas sections showing proliferating cells in an islet (G) and in acinar tissue (H) (original magnification $\times 200$). The arrows indicate double-positive cells. I: Model depicts FoxM1 regulation of optimal β -cell function and proliferation.

elevated proliferation and increased β -cell mass. The ability to increase β -cell replication in aged islets is particularly important because aged β -cells are recalcitrant to replicative stimuli and because T2D onset increases with age in humans.

Previous successful efforts to increase β -cell replication in aged islets have included elimination or indirect downregulation of p16 in mouse islets (10,28) or downregulation of the cell-cycle inhibitor p57 in human islets (38). Considering that all successful endeavors to increase β -cell

mass in aged mice have involved decreasing p16 and that FoxM1 negatively regulates p16 expression in other cell types, we expected p16 to be decreased in aged β -cells expressing activated FoxM1 and displaying increased β -cell mass and proliferation. Contrary to these expectations, no change in p16 was observed in activated FoxM1-expressing cells. However, the senescence and DNA damage marker γ -H2AX was decreased in β -FoxM1* mice without any change in TUNEL⁺ cells, indicating that activated FoxM1 is bypassing p16 to permit aged β -cells to reenter the cell cycle. Alternatively, most of the β -cell replication, and thus the decrease in p16, could have occurred soon after activated FoxM1 induction rather than at the 2-week point examined here. At 12 months, the expansion in β -cell mass 2 weeks after FoxM1 induction is substantial in the absence of any increase in ad libitum-fed blood glucose, suggesting that these mice are probably not insulin resistant and that elevated blood glucose is not responsible for the increased β -cell proliferation. Compared with the increase in β -cell mass, the elevation in β -cell replication in 12-month-old β -FoxM1* mice is less impressive. This smaller-than-expected elevation in β -cell proliferation may reflect negative feedback inhibition on the cell cycle by the 2-week time point examined; β -cell proliferation may have been much higher just after initiating activated FoxM1 expression.

At 2 months of age, before any elevation in β -cell mass, β -FoxM1* mice display improved glucose homeostasis, suggesting that FoxM1 regulates insulin secretion. We further showed that activated FoxM1 is acting cell autonomously upstream of Ca^{2+} influx and downstream of insulin production to enhance insulin secretion.

In retrospect, a role for FoxM1 in β -cell function should not have been surprising because previous work from our laboratory demonstrated that male mice lacking FoxM1 in the pancreas displayed diabetes or glucose intolerance with only a 60% decrease in β -cell mass (15) and that mice expressing activated FoxM1 display improved blood glucose in response to streptozotocin treatment before any improvement in β -cell mass (19). In addition, many mouse models can support a decrease in β -cell mass of 80% or more and still maintain glucose homeostasis (39). Furthermore, maintenance of euglycemia with a severe reduction in β -cell mass echoes what is observed in the progression toward type 1 diabetes: patients display the most severe symptoms only after a loss in β -cell mass $>90\%$ (40). We therefore examined insulin secretion in size-matched islets from mice lacking FoxM1 specifically in β -cells and demonstrated that these islets secreted less insulin than control islets despite normal insulin content, confirming a previously unappreciated role for FoxM1 in the regulation of β -cell function. No increase in circulating insulin was observed during a glucose tolerance test in mice expressing activated FoxM1, however, which may indicate a faster disposal of insulin in peripheral tissues.

In pancreatic acinar cells, FoxM1 can only be detected within proliferating cells, but while FoxM1 is expressed at high levels in proliferating islet cells, it is also expressed at lower levels in all other islet cells. We propose a model in which FoxM1 is required for β -cell function, activating genes involved in this process at low protein levels, but to surpass the threshold for cell-cycle entry, FoxM1 must be expressed at higher levels (Fig. 7I). Taken together, our data indicate that changes in glucose homeostasis in β -FoxM1* mice are at least partially decoupled from increases in β -cell mass. Future studies will investigate how FoxM1 distinguishes its proliferative versus functional targets in the β -cell.

Our experiments indicate that FoxM1 acts cell autonomously to enhance β -cell proliferation and function, but we reported previously that only ~10% of β -cells express activated FoxM1 in β -FoxM1* mice (19). How, then, can gene expression changes in such a low proportion of β -cells translate to such a large change in β -cell mass in just 2 weeks? RIP-rtTA generally drives expression of its targets in a large percentage of β -cells. Unlike many proteins, however, endogenous expression of FoxM1 is dynamically regulated with the cell cycle, and although the HA-FoxM1^{ΔNRD} transgene lacks a domain that directs FoxM1 to the proteasome, FoxM1 degradation may have additional layers of control. Activated FoxM1 may be expressed in only 10% of β -cells at any given time point, but the pool of β -cells in which activated FoxM1 is expressed may be greater over time.

Much attention in the field of β -cell proliferation has focused on extracellular factors because they might be easier to modulate than intracellular factors. However, recent work has suggested that human β -cells are less responsive to extracellular growth factors than mouse β -cells because of reduced expression of receptors for these growth factors, especially with age (41–43). We show that activation of FoxM1 in aged β -cells can bypass inherent brakes present in these cells while enhancing function. Successful drugs inhibiting FOXM1 are on the market today (44), demonstrating the feasibility of targeting FOXM1 activity in vivo and suggesting that FoxM1 is a worthwhile therapeutic target for T2D.

Acknowledgments. The authors thank Dr. Marcela Brissova, Greg Poffenberger, Anastasia Coldren, and Wendell Nicholson (all at Vanderbilt University) for technical assistance.

Funding. This work was supported by the U.S. Department of Veterans Affairs (grant 1BX000990-01A1 to M.G.) and JDRF (grant 3-2010-563 to M.L.G.). M.L.G. was also supported by the National Cancer Institute (Integrated Biological Systems Training in Oncology Training Grant 5T32 CA119925). D.A.J. was supported by the National Institute of Diabetes and Digestive and Kidney Diseases (DK-97392). The Transgenic/ES Cell Shared Resource and the Islet Procurement & Analysis Core of the Vanderbilt Diabetes Research and Training Center are supported by National Institutes of Health (NIH) grant DK-20593. Data presentation was performed in part through the use of the Cell Imaging Shared Resource of the Vanderbilt Diabetes Research and Training Center,

supported by NIH grants CA-68485, DK-20593, DK-58404, DK-59637, and EY-08126. The Hormone Assay & Analytical Services Core of the Vanderbilt Diabetes Research and Training Center is supported by NIH grants DK-59637 and DK-20593.

Duality of Interest. No potential conflicts of interest relevant to this article were reported.

Author Contributions. M.L.G. designed and performed experiments, analyzed data, and wrote the manuscript. J.C.D., M.F.M., and P.K.D. performed experiments. A.B.O. and M.A.M. assisted with the experimental design and edited the manuscript. D.A.J. assisted with the experimental design, analyzed data, contributed to discussion, and edited the manuscript. M.G. assisted with the experimental design, analyzed data, and wrote the manuscript. M.G. is the guarantor of this work and, as such, had full access to all the data in the study and takes responsibility for the integrity of the data and the accuracy of the data analysis.

Prior Presentation. Parts of this study were presented in the President's Oral Sessions at the 75th Scientific Sessions of the American Diabetes Association, Boston, MA, 5–9 June 2015.

References

- Mendis S. *Global Status Report on Noncommunicable Diseases 2014*. Geneva, WHO Press, 2014, p. 98
- Rahier J, Guiot Y, Goebbels RM, Sempoux C, Henquin JC. Pancreatic beta-cell mass in European subjects with type 2 diabetes. *Diabetes Obes Metab* 2008; 10(Suppl. 4):32–42
- Butler AE, Janson J, Bonner-Weir S, Ritzel R, Rizza RA, Butler PC. Beta-cell deficit and increased beta-cell apoptosis in humans with type 2 diabetes. *Diabetes* 2003;52:102–110
- Centers for Disease Control and Prevention. *National Diabetes Statistics Report: Estimates of Diabetes and Its Burden in the United States 2014*. Atlanta, Georgia, Centers for Disease Control and Prevention, 2014, p. 1
- Meier JJ, Butler AE, Saisho Y, et al. Beta-cell replication is the primary mechanism subserving the postnatal expansion of beta-cell mass in humans. *Diabetes* 2008;57:1584–1594
- Reers C, Erbel S, Esposito I, et al. Impaired islet turnover in human donor pancreata with aging. *Eur J Endocrinol* 2009;160:185–191
- Gregg BE, Moore PC, Demozay D, et al. Formation of a human β -cell population within pancreatic islets is set early in life. *J Clin Endocrinol Metab* 2012;97:3197–3206
- Teta M, Rankin MM, Long SY, Stein GM, Kushner JA. Growth and regeneration of adult beta cells does not involve specialized progenitors. *Dev Cell* 2007;12:817–826
- Rankin MM, Kushner JA. Adaptive beta-cell proliferation is severely restricted with advanced age. *Diabetes* 2009;58:1365–1372
- Krishnamurthy J, Ramsey MR, Ligon KL, et al. p16INK4a induces an age-dependent decline in islet regenerative potential. *Nature* 2006;443:453–457
- Tschen SI, Dhawan S, Gurlo T, Bhushan A. Age-dependent decline in beta-cell proliferation restricts the capacity of beta-cell regeneration in mice. *Diabetes* 2009;58:1312–1320
- Liu Y, Mziaut H, Ivanova A, Solimena M. beta-Cells at the crossroads: choosing between insulin granule production and proliferation. *Diabetes Obes Metab* 2009;11(Suppl. 4):54–64
- Li SK, Smith DK, Leung WY, et al. FoxM1c counteracts oxidative stress-induced senescence and stimulates Bmi-1 expression. *J Biol Chem* 2008;283:16545–16553
- Wang IC, Chen YJ, Hughes D, et al. Forkhead box M1 regulates the transcriptional network of genes essential for mitotic progression and genes encoding the SCF (Skp2-Cks1) ubiquitin ligase. *Mol Cell Biol* 2005;25:10875–10894
- Zhang H, Ackermann AM, Gusarova GA, et al. The FoxM1 transcription factor is required to maintain pancreatic beta-cell mass. *Mol Endocrinol* 2006;20:1853–1866
- Zhang H, Zhang J, Pope CF, et al. Gestational diabetes mellitus resulting from impaired beta-cell compensation in the absence of FoxM1, a novel downstream effector of placental lactogen. *Diabetes* 2010;59:143–152

17. Ackermann Misfeldt A, Costa RH, Gannon M. Beta-cell proliferation, but not neogenesis, following 60% partial pancreatectomy is impaired in the absence of FoxM1. *Diabetes* 2008;57:3069–3077
18. Davis DB, Lavine JA, Suhonen JI, et al. FoxM1 is up-regulated by obesity and stimulates beta-cell proliferation. *Mol Endocrinol* 2010;24:1822–1834
19. Golson ML, Maulis MF, Dunn JC, et al. Activated FoxM1 attenuates streptozotocin-mediated β -cell death. *Mol Endocrinol* 2014;28:1435–1447
20. Milo-Landesman D, Surana M, Berkovich I, et al. Correction of hyperglycemia in diabetic mice transplanted with reversibly immortalized pancreatic beta cells controlled by the tet-on regulatory system. *Cell Transplant* 2001;10:645–650
21. Postic C, Shiota M, Niswender KD, et al. Dual roles for glucokinase in glucose homeostasis as determined by liver and pancreatic beta cell-specific gene knock-outs using Cre recombinase. *J Biol Chem* 1999;274:305–315
22. Wang X, Kiyokawa H, Dennewitz MB, Costa RH. The forkhead box m1b transcription factor is essential for hepatocyte DNA replication and mitosis during mouse liver regeneration. *Proc Natl Acad Sci U S A* 2002;99:16881–16886
23. Chen SX, Osipovich AB, Ustione A, et al. Quantification of factors influencing fluorescent protein expression using RMCE to generate an allelic series in the ROSA26 locus in mice. *Dis Model Mech* 2011;4:537–547
24. Zhang H, Ables ET, Pope CF, et al. Multiple, temporal-specific roles for HNF6 in pancreatic endocrine and ductal differentiation. *Mech Dev* 2009;126:958–973
25. Golson ML, Bush WS, Brissova M. Automated quantification of pancreatic β -cell mass. *Am J Physiol Endocrinol Metab* 2014;306:E1460–E1467
26. Golson ML, Ackermann AM, Kopsunbut UG, Petersen CP, Gannon MA. High fat diet regulation of β -cell proliferation and β -cell mass. *Open Endocrinol J* 2010;4:66–77
27. Laoukili J, Kooistra MR, Brás A, et al. FoxM1 is required for execution of the mitotic programme and chromosome stability. *Nat Cell Biol* 2005;7:126–136
28. Zhou JX, Dhawan S, Fu H, et al. Combined modulation of polycomb and trithorax genes rejuvenates β cell replication. *J Clin Invest* 2013;123:4849–4858
29. Rodier F, Muñoz DP, Teachenor R, et al. DNA-SCARS: distinct nuclear structures that sustain damage-induced senescence growth arrest and inflammatory cytokine secretion. *J Cell Sci* 2011;124:68–81
30. Brouwers B, de Faudeur G, Osipovich AB, et al. Impaired islet function in commonly used transgenic mouse lines due to human growth hormone minigene expression. *Cell Metab* 2014;20:979–990
31. Lee JY, Ristow M, Lin X, White MF, Magnuson MA, Hennighausen L. RIP-Cre revisited, evidence for impairments of pancreatic beta-cell function. *J Biol Chem* 2006;281:2649–2653
32. Komatsu M, Takei M, Ishii H, Sato Y. Glucose-stimulated insulin secretion: a newer perspective. *J Diabetes Investig* 2013;4:511–516
33. Korver W, Roose J, Clevers H. The winged-helix transcription factor Trident is expressed in cycling cells. *Nucleic Acids Res* 1997;25:1715–1719
34. Laoukili J, Alvarez-Fernandez M, Stahl M, Medema RH. FoxM1 is degraded at mitotic exit in a Cdh1-dependent manner. *Cell Cycle* 2008;7:2720–2726
35. Marroquí L, Gonzalez A, Neco P, et al. Role of leptin in the pancreatic β -cell: effects and signaling pathways. *J Mol Endocrinol* 2012;49:R9–R17
36. Krupczak-Hollis K, Wang X, Kalinichenko VV, et al. The mouse forkhead box m1 transcription factor is essential for hepatoblast mitosis and development of intrahepatic bile ducts and vessels during liver morphogenesis. *Dev Biol* 2004;276:74–88
37. Ma RY, Tong TH, Cheung AM, Tsang AC, Leung WY, Yao KM. Raf/MEK/ MAPK signaling stimulates the nuclear translocation and transactivating activity of FOXM1c. *J Cell Sci* 2005;118:795–806
38. Avrahami D, Li C, Yu M, et al. Targeting the cell cycle inhibitor p57Kip2 promotes adult human β cell replication. *J Clin Invest* 2014;124:670–674
39. Golson ML, Loomes KM, Oakey R, Kaestner KH. Ductal malformation and pancreatitis in mice caused by conditional Jag1 deletion. *Gastroenterology* 2009;136:1761–1771 e1761
40. Matveyenko AV, Butler PC. Relationship between beta-cell mass and diabetes onset. *Diabetes Obes Metab* 2008;10(Suppl. 4):23–31
41. Chen H, Gu X, Liu Y, et al. PDGF signalling controls age-dependent proliferation in pancreatic β -cells. *Nature* 2011;478:349–355
42. Kulkarni RN, Mizrachi EB, Ocana AG, Stewart AF. Human β -cell proliferation and intracellular signaling: driving in the dark without a road map. *Diabetes* 2012;61:2205–2213
43. Bernal-Mizrachi E, Kulkarni RN, Scott DK, Mauvais-Jarvis F, Stewart AF, Garcia-Ocaña A. Human β -cell proliferation and intracellular signaling part 2: still driving in the dark without a road map. *Diabetes* 2014;63:819–831
44. Gormally MV, Dexheimer TS, Marsico G, et al. Suppression of the FOXM1 transcriptional programme via novel small molecule inhibition. *Nat Commun* 2014;5:5165